Contents

1. List of Experiments
2. Product Determination
3. Parametrization of Reaction Kinetics

1 List of Experiments

Table S1. List of experiments performed and their chemical characteristics. Solution nomenclature is carried out through the supplemental information. Nuclear magnetic resonance (NMR) spectroscopy measurements were taken with 500 MHz 1H-NMR with 64 scans per measurement. $[BD]_0$ and $[NH_X]_0$ were determined from the mass of each species added to the mixtures. pH was estimated with in-situ quantitative measurements of the NMR shift of an acid.

Solution	Measurement	$[BD]_0$ (M)	$[NH_X]_0$ (M)	pH	Comment
BD_H2O_02	NMR	0.02	0	3[3]	Butenedial isomer analysis
BD_H2O_25	NMR	0.25	0	3[3]	Butenedial isomer analysis
BD_H2O_09	NMR	0.09	0	3[3]	Butenedial acetal formation
BD_H2O_55	NMR	0.55	0	3[3]	Butenedial acetal formation
BD_OH_pH8.8	NMR	0.2	0	8.8	R1 Fitting
BD_OH_pH9.5	NMR, MS[2]	0.2	0	9.5	R1 Fitting
BD_OH_pH9.8	NMR	0.2	0	9.8	R1 Fitting
BD_OH_pH10.4	NMR	0.2	0	10.4	R1 Fitting
BD_NH_pH3.6	NMR	0.4	0.4	3.6	Mechanism Validation
BD_NH_pH5	NMR, MS[1]	0.9	0.9	4.2-5.7	R2-R6 Fitting
BD_NH_pH8.5	NMR	0.9	0.2	8.5-8.8	Mechanism Validation

[1]The mass spectrometry (MS) spectra for BD_NH_pH5 was taken with a commercial time-of-flight mass spectrometer (JEOL AccuTOF) in positive ion mode only. [2]The MS spectra for BD_OH_pH9.5 was taken with liquid chromatography – mass spectrometry in negative ion mode direct injection. [3]These pH measurements were taken with litmus paper.

2 Molecular Identification and Quantification

2.i Methodology

The solutions BD_NH_pH5 and BD_OH_pH9.5 were analyzed to identify reactants and products during reaction. Solutions with identical initial conditions were analyzed separately with MS and 1H-NMR, aside from the addition of internal standards added to solution to enable quantitation and pH estimation in the case of NMR.

MS measurements of each solution were recorded to identify the molecular formula of major reaction products. Hexaethylene glycol (PEG-6) was added to BD_NH_pH5 as an internal standard. We did not identified interactions between butenedial and PEG-6 in a previous study (Birdsall et al., 2019). No internal standard was added to BD_OH_pH9.5 for MS analysis.

NMR was performed quantitatively using dilute (1-2% w/w) dimethyl sulfone (DMS) or diethylmalonic acid (DEM) as an internal standard, added to the solution. Concentrations of identified species were calculated with the relative signal intensity of their protons against that of DMS, as is described elsewhere (e.g., Yu et al., 2011). Areas of integration were estimated with MestReNova's line fitting software. The 1H-NMR spectra showed distinct groups of quantitative related signals that had similar temporal behavior. Each group of peaks whose quantitative signal strength behaved as integers and had the same temporal behavior was presumed to arise from a single compound. A molecular structure was proposed for each cluster of peaks and the molecular formulas mentioned above. In most cases, the quantitation was performed with a subset of the total peaks belonging to a molecule to avoid distortions from neighboring peaks and the background.

2.ii Butenedial in H_2O

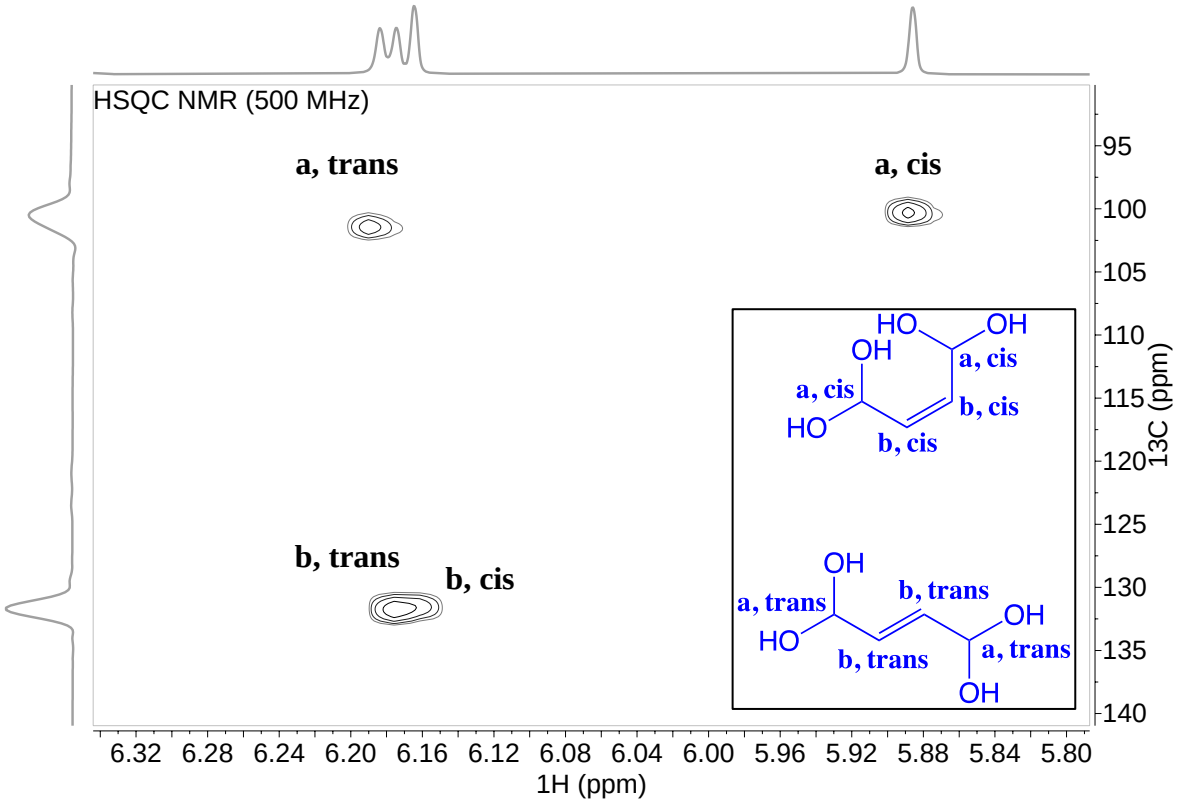

Figure S1. HSQC NMR spectrum of concentrated (~0.5 M) butenedial in D_2O. Butenedial (BD, $C_4H_8O_4$) is shown in the inset as a dihydrate, the dominant form of butenedial observed in aqueous solution, as both the cis and the trans isomer. The protons are assigned, according to their alphabetical labels, for both the cis and trans isomer. The proton with chemical shifts 6.17 and 5.86 ppm are assigned to the gem-diol carbon. The protons with chemical shifts 6.16 and 6.15 ppm are assigned to the alkene carbon. The upfield protons of each carbon are assigned to the cis isomer, and the downfield protons to the trans isomer, as is typical. Unhydrated BD was detected with MS at the m/z 85 channel.

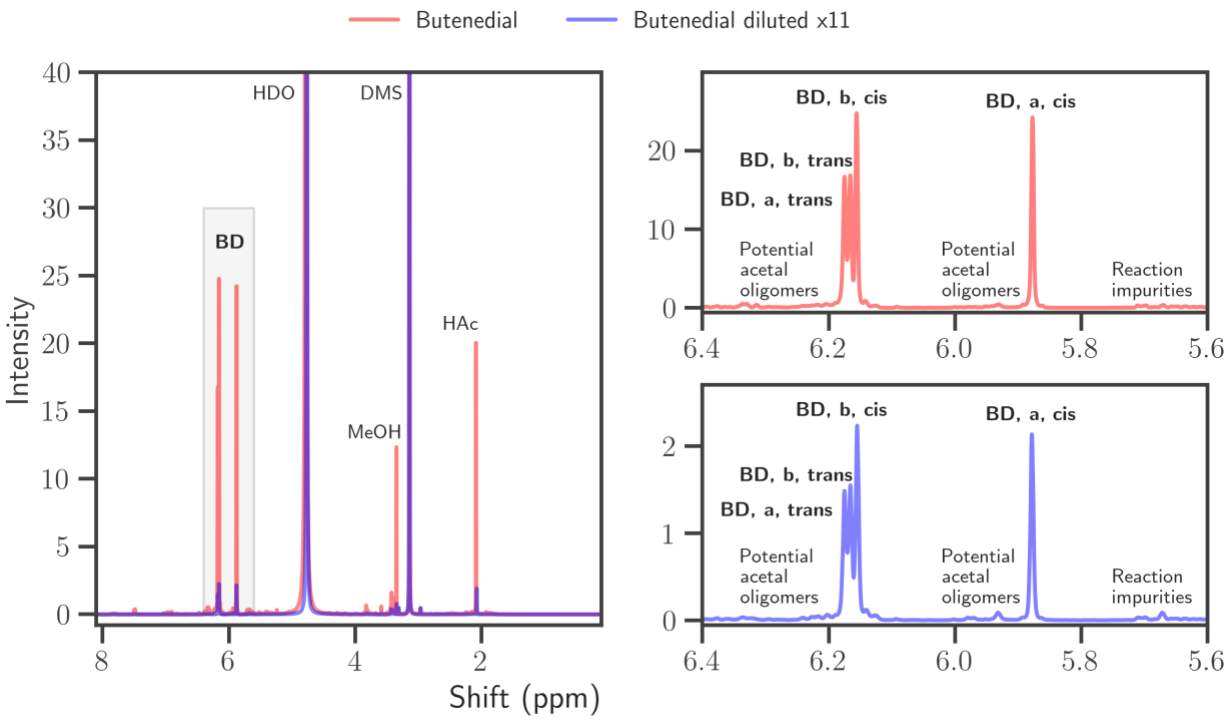

Figure S2. Species assignments in 1H-NMR spectra of the BD_H2O solutions, where one spectrum is taken of a solution (blue, BD_H2O_25) from an eleven-fold dilution of the other (red, BD_H2O_02). An overview spectrum is plotted to the left, and two expanded regions, identified by the shaded box, are plotted on the right for each of the spectra. Major peaks are labeled with their associated chemical compounds and corresponding protons (see Figure S1). The broad singlet at 4.76 is HDO (deuterium substituted water) solvent signal. Dimethyl sulfone (DMS) was the internal standard used as a reference and for quantitation. Acetic acid (HAc) is a nonreactive impurity from butenedial synthesis. Methanol (MeOH) is also detected as a nonreactive byproduct of the reaction.

Table S2. Reported quantitation of BD protons (see Figure S3) in BD_H2O solutions. Intensity (I) is reported assuming I(DMS) = 100. The ratio of cis to trans is near to unity.

Proton	Intensity (BD_H2O_25)	Intensity (BD_H2O_02)
BD, a, cis	25.8	2.8
BD, b, cis	25.0	2.6
BD, a, trans	20.0	2.4
BD, b, trans	25.0	2.2

Quantification of butenedial acetal oligomerization.

Table S3. Reported quantitation of BD_H2O_55 and BD_H2O_09 solutions. Three BD_H2O_55 solutions were each diluted approximately six-fold to BD_H2O_09 solutions, according to the

nominal dilution factor reported. The BD dihydrate molarities, measured in-situ, are provided as a comparison against the nominal dilution factor between pairs, to demonstrate if hydration speciation depends on BD concentration. The *maximum* BD acetal oligomer concentration is also presented, which was calculated by assigning the integrated signal intensity between 6.5-6.25 ppm and 6.15-5.9 ppm to a BD acetal dimer (with 8 assignable protons in this range). All values are given as averages and their standard deviations.

Solution	Measured [BD dihydrate]	Dilution factor	Measured max [BD acetal oligomer]
BD_H2O_55	0.55 ± 0.03 M	NA	0.023 ± 0.002 M
BD_H2O_09	0.089 ± 0.012 M	5.86 ± 0.12	0.003 ± 0.0005 M

Fratzke et al. (1985) define the equilibrium between monomer and hydrate dimer according to the following relation:

$$K = \frac{[D]}{[M]^2}$$

Where [D] is the hydrated dimer concentration and [M] is the monomer (hydrated or unhydrated) concentration. For glyoxal, K is reported to be 0.56 M^{-1} (Fratzke and Reilly, 1986). This results in a dimer concentration of 170 mM at a glyoxal monomer concentration of 0.55 M. Table S2 shows that the maximum butenedial acetal oligomer concentration can be at most 23 mM with 0.55 M butenedial dihydrate. This assumes that all signal specified in the caption to Table S2 corresponds to acetal oligomers and suggests that a tentative upper bound of the K estimate for butenedial is 0.08 M^{-1}. However, dilution experiments provide strong evidence that only a very small fraction of this signal corresponds to BD acetal oligomers:

If acetal dimers are formed, a dilution of butenedial solution leads to (1) a statistically significant decrease in butenedial concentration relative to the dilution factor and (2) a quadratic decrease in the dimer concentration compared to the butenedial monomer concentration.

1. The relative butenedial molarity of BD_H2O_55 to BD_H2O_09 is 6.28 ± 1.20 : 1 and the nominal dilution factor is 5.86 ± 0.12 (determined via the non-reactive standard). Thus, we do not find a significant difference between the nominal and measured concentration of butenedial dihydrate after dilution.
2. The decrease in maximum BD acetal oligomer concentration is 7.31 ± 1.43 from the dilution, which is far from quadratic with respect to the butenedial dihydrate decrease (which would be a factor of ~39). In addition, the upper limit of the observed BD acetal oligomer concentration post dilution, 0.0035M, is identical to the value calculated for the BD acetal oligomer concentration using upper limit of the dilution factor, 5.98, and the lower limit of the observed BD acetal oligomer concentration pre dilution, 0.021M. This indicates that the signal is predominantly from other compounds than acetal oligomers, which should equilibrate rapidly based on analysis of glyoxal acetal oligomers and general chemical considerations.

We therefore find that the presence of butenedial acetal oligomers is minimal, and clearly much less pronounced than for glyoxal.

2.iii Butenedial + OH^- Reaction

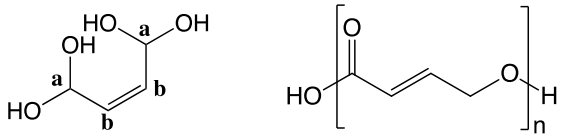

Butenedial (BD) **γ-hydroxycrotonic acid (GHC) oligomer**

$C_4H_8O_4$ $[C_4H_4O_2]_n(H_2O)$

m/z 85 m/z 17 + 84n

Figure S3. Butenedial (BD) and γ-hydroxycrotonic acid (GHC) oligomer structures are shown in the figure above. GHC is an observed reaction product of the BD/OH^- reaction, which is analogous to other dicarbonyl disproportionation reactions, e.g., glyoxal to glycolic acid. GHC was not explicitly identified with NMR. The mass-to-charge (m/z) ratios of each species are given. BD dihydrate is the dominant form of BD observed in aqueous solutions. Unhydrated BD was detected with MS and the m/z ratio of its unhydrated forms is reported. The m/z ratios of deprotonated GHC are provided as they were the species detected with MS.

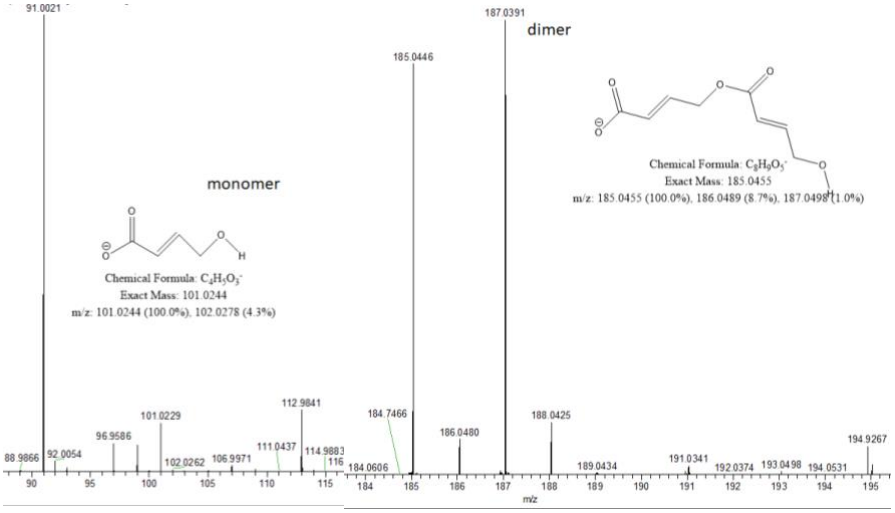

Figure S4. Mass spectrum taken of BD_OH_pH9.5 after approximately thirty minutes of reaction, m/z channels 90-115 (left panel) and 182-197 (right panel). Plots are not on equal scales. GHC monomer (m/z 101) and dimer (m/z 185) are observed.

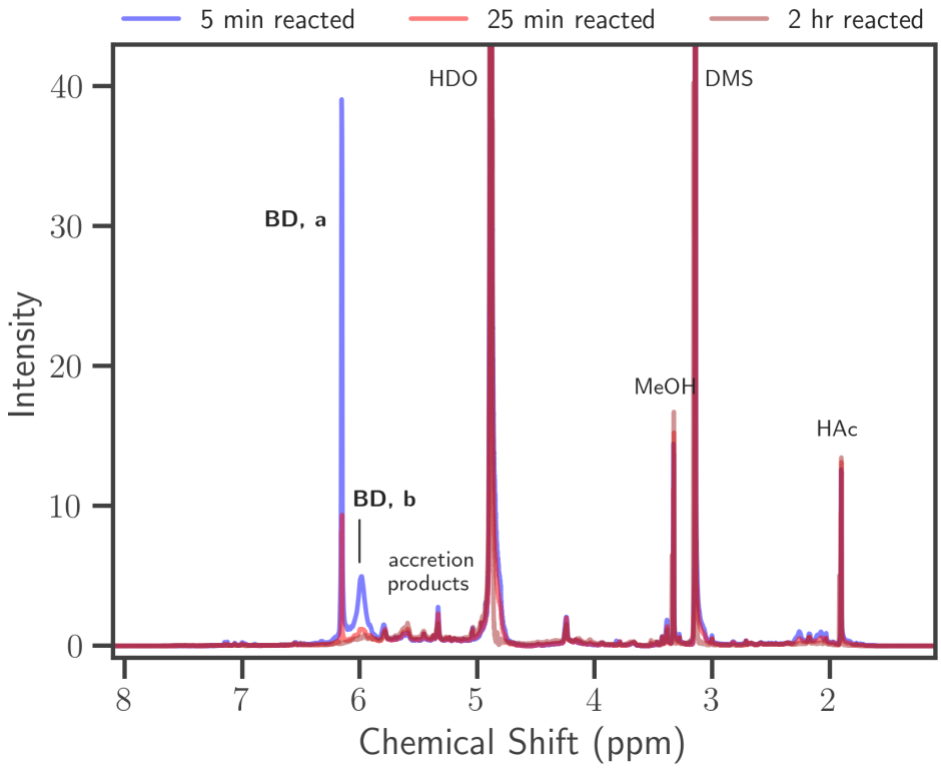

Figure S5. Product assignments in 1H-NMR spectra of the BD_OH solution, recorded 5 min (blue), 25 min (red), and 2 hr (brown) after mixing. An overview spectrum is plotted on top, and two expanded regions, identified by the shaded boxes, are plotted on bottom. Major peaks are labeled with their associated chemical compounds and corresponding protons (see Figure S3). The proton used for quantitation is identified with a bolded label. The butenedial gem diol protons are collapsed to one broad peak, as they may be exchanging with the solvent. The broad singlet at 4.76 is HDO (deuterium substituted water) solvent signal. Dimethyl sulfone (DMS) was the internal standard used as a reference and for quantitation. Acetic acid (HAc) is a nonreactive impurity from butenedial synthesis. Methanol (MeOH) is also detected as a nonreactive byproduct of the reaction. The buildup of the baseline at ~6.2-5 and ~4.5-3.6 ppm is expected to be from accretion reactions.

δ (ppm) of *butenedial dihydrate*: 6.15, 5.96

Notes on quantitation. For BD, the gem diol protons are less affected by the background than the alkene protons, and was therefore used in the quantitation, assuming a 2:1 gem diol to butenedial molar ratio.

Table S4. Reported quantitation of BD protons (see Figure S5) in BD_OH_pH10.4 solution at 5 min, 25 min, and 2 hr of reaction. Intensity (I) is reported assuming I(DMS) = 100. Intensities are insignificant of butenedial at 2 hr reaction. Near integer relationship between the two protons is observed.

Proton	Intensity	Intensity	Intensity

	(5 min)	(25 min)	(2 hr)
BD, a	0.425	0.141	0
BD, b	0.488	0.142	0

2.iv Butenedial + NH_X Reaction

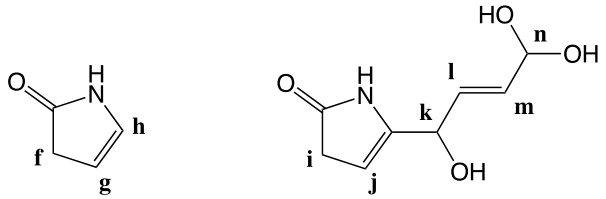

Pyrrolinone (PR)

C_4H_5ON
m/z 84

Butenedial-pyrrolinone dimer (BD-PR)

$C_8H_{11}O_4N$
m/z 168

Figure S6. Pyrrolinone (PR) and butenedial-pyrrolinone dimer (BD-PR) structures are shown in the figure above. BD-PR hydrate is the dominant forms of BD-PR observed in aqueous solutions. Unhydrated BD-PR was detected with MS and the m/z ratio of its unhydrated forms is reported. PR and BD-PR are the major reaction products of the BD/NH_X reaction. The observed mass-to-charge (m/z) ratios of each species are given for adducts with H^+. The protons identified with NMR are labeled alphabetically for those attached to carbon atoms.

Butenedial/NH_X Reaction. We tentatively propose that butenedial/NH_X reaction proceeds as follows, although reaction intermediates are not observed with NMR or MS. Reaction begins when NH_3 attacks a protonated carbonyl carbon, forming an unstable hemiaminal that dehydrates to produce an imine. The imine can undergo ring closure, forming a hydroxypyrrole. The hydroxypyrrole is in equilibrium with pyrrolinone, which is the stable and favored form in an aqueous medium (Bocchi et al., 1970; Bordner and Rapoport, 1965; Hill et al., 2009). The ketonization of hydroxy heterocycles has been shown to increase with decreasing pH (Capon et al., 1987). As such, the tautomerization of pyrrolinone to the reactive hydroxypyrrole would be OH^--dependent. The proposed dimerization of butenedial with pyrrolinone takes place at the carbon adjacent to the NH group, as is typical for aldehyde/pyrrole reactions, e.g., in porphyrin synthesis (Koelsch and Richter, 1935).

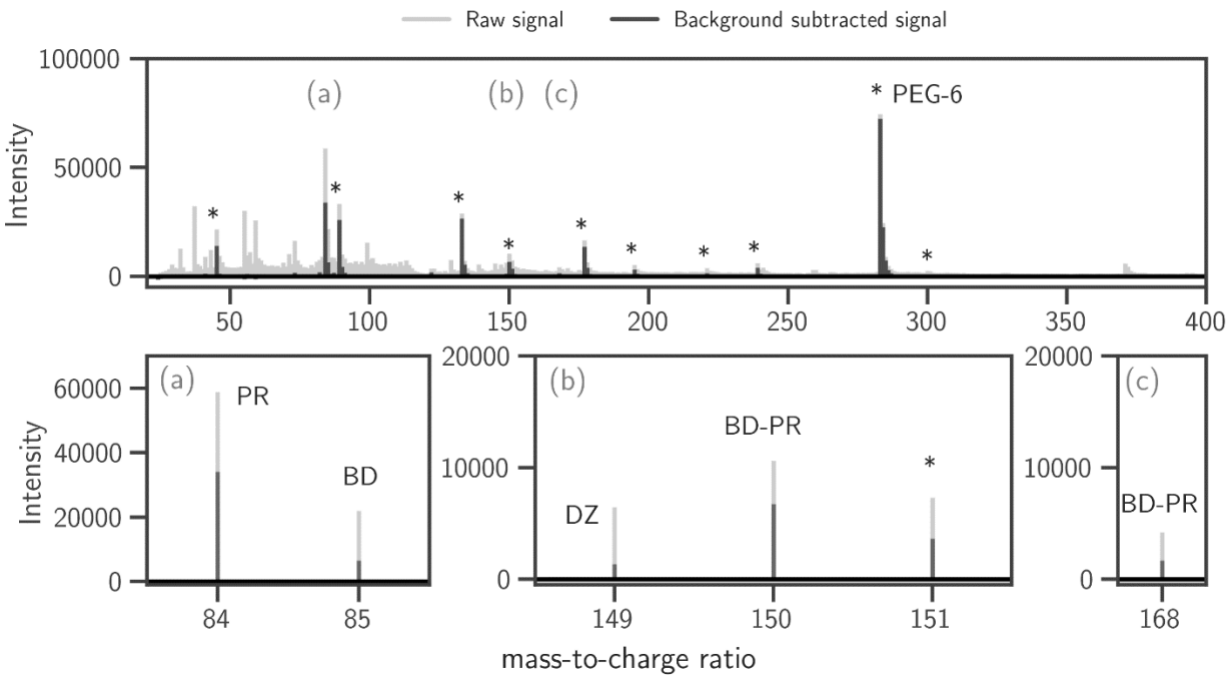

Figure S7. Spectrum of BD_NH_pH5 solution after ~20 minutes of reaction. Raw (gray) and background-subtracted (black) mass spectra are provided. The full spectrum is shown on the top panel, with lettered expanded regions on the bottom that demonstrate reactant and products. All species observed form adducts with H^+. Starred peaks correspond to PEG-6, its fragments, and clusters of water with PEG-6 and its fragments. These fragments were identified in previous studies (Birdsall et al., 2018, 2019). The background signal is residual from the experimental apparatus.

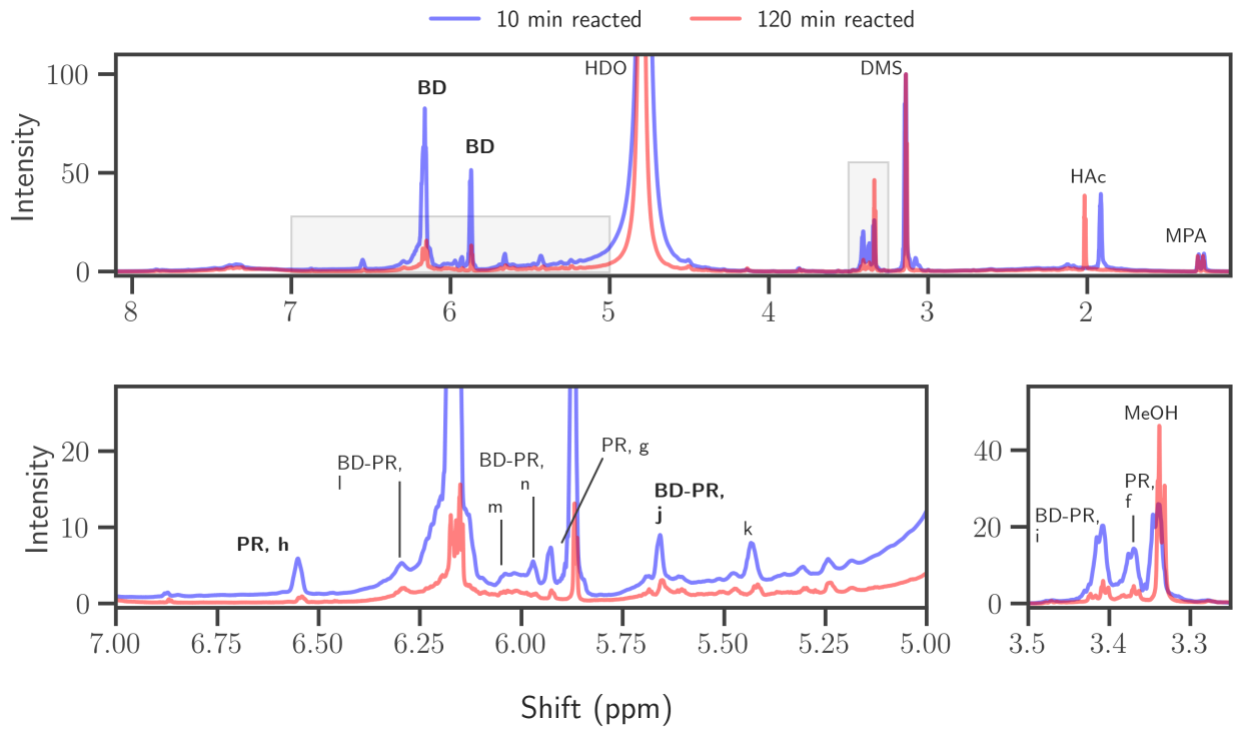

Figure S8. Product assignments in 1H-NMR spectra of the BD_NH_pH5 solution, recorded after 10 min (blue) and 120 min (red) of reaction. An overview spectrum is plotted on top, and two expanded regions, identified by the shaded boxes, are plotted on bottom. Major peaks are labeled with their associated chemical compounds and corresponding protons (see Figure S6). Asterisked labels indicate a proton in the cis or trans isomer. The proton used for quantitation is identified with a bolded label. The broad singlet at 4.76 is HDO (deuterium substituted water) solvent signal. Dimethyl sulfone (DMS) was the internal standard used as a reference and for quantitation. Methylphosphonic acid (MPA) was the internal standard used in conjunction with acetic acid (HAc), a nonreactive impurity from butenedial synthesis, for pH estimation. The change in HAc chemical shift observed between the two spectra is due to speciation changes from acid-base equilibrium. Methanol (MeOH) is also detected as a nonreactive byproduct of the reaction.

δ (ppm) of reactants and products. *Butenedial dihydrate*: 6.17, 6.16, 6.15, 5.86; *pyrrolinone*: 6.55, 5.92, 3.37; *butenedial-pyrrolinone dimer hydrate*: 6.29, 6.03, 5.97, 5.65, 5.43, 3.41.

Table S5. Reported quantitation of BD, PR, and BD-PR protons (see Figure S6) in BD_NH_pH5 solution at 10 minutes and 120 minutes of reaction. Intensity (I) is reported assuming I(DMS) = 100. Intensity of protons from the cis and trans isomer are provided as tuples. In general, proximity to integer relationships is maintained across protons of a species through time. The NH proton was not used in quantitation.

Proton	Intensity (10 min)	Intensity (120 min)
BD, cis	69	14

BD, trans	56	11
PR, f	18	3.7
PR, g	7.4	2.0
PR, h	11	2.0
BD-PR, i	32	9.0
BD-PR, j	14	4.0
BD-PR, k	12	4.3
BD-PR, l	12	4.0
BD-PR, m	10	N/A[1]
BD-PR, n	12	N/A[1]

[1]The signal of these protons of BD-PR was not resolved with the integration software at 120 minutes, presumably due to overlapping signal.

Notes on quantitation. For BD, the total proton signal was used to perform the quantitation when the BD signal was sufficiently higher than the background, approximately 10 intensity units. The upfield gem-diol proton (a, cis) is less affected by the background than the other protons, and it is observed that the ratio of cis to trans (~0.55/0.45) is constant during reaction. At low BD signal intensity, the BD quantitation was performed by multiplying the upfield gem-diol proton (a, cis) signal by 1.8 to obtain total butenedial concentration, both cis and trans forms. PR quantitation was performed with the downfield alkene proton (h). BD-PR quantitation was performed with the heterocyclic alkene proton (j).

2.v Images of aqueous solutions during reaction

Figure S9. BD_OH_pH8.8 (left) and BD_OH_pH10.4 (right) solutions in an NMR tube after ~40 minutes of reaction. A color change was immediate. No solids were observed in BD_OH_pH8.8, BD_OH_pH9.5, BD_OH_pH9.8, or BD_OH_pH10.4 solutions.

Figure S10. Series of 0.4 M BD/0.2 M AS solutions at increasing time of reaction rightward (left). 0.4 M BD/0.2 M AS solution after weeks of reaction (right). Solutions had approximately the same starting composition. The solutions darken over time and solids appear to form. A visible color change to a darker yellow was observed within minutes. Black-brown color was noticeable after hours of reaction. The accumulation of solids occurred on longer timescales (many hours to days). Solids were also observed rapidly (under an hour) in BD/NH_X solutions with higher pH (e.g., in BD_NH_pH8.5 experiments).

3. Parametrizations

3.i pH estimation with NMR

pH estimation with 1H-NMR is described elsewhere in detail (Wallace et al., 2018). In brief, dilute (<1% w/w) acid is added to solution, and selected such that its pKa ~ solution pH ± 2. Acetic acid is present as an impurity in the starting material and is also used as a pH indicator. The acids used are described in Table S5. pH is calculated from the recorded chemical shift (δ) of the acid via the equation below, where δ_{A-} and δ_{HA} are the chemical shifts of the deprotonated and protonated acid, respectively. δ_{A-} and δ_{HA} were recorded in this study and closely match those reported by Wallace et al. (2018).

$$pH = pKa + log_{10}\left(\frac{\delta_{A-} - \delta}{\delta_{A-} - \delta_{HA}}\right)$$

Table S6. pH indicator, relevant quantities, and use in experimental runs of this work.

Indicator	pKa	δ_{A-}	δ_{HA}	Experiments used
Acetic acid	4.58[1]	1.90	2.09	BD_NH_pH5, BD_NH_pH3.6
Methylphosphonic acid	7.78[1]	1.07	1.29	BD_OH_pH8.8, BD_OH_pH9.5, BD_NH_pH8.5
2,4,6-trimethylphenol	10.88[2]	6.36	6.62	BD_OH_pH9.8, BD_OH_pH10.4

[1]Values given by Wallace et al. (2018). [2] Retrieved from: National Center for Biotechnology Information. PubChem Compound Summary for CID 10698, 2,4,6-Trimethylphenol. https://pubchem.ncbi.nlm.nih.gov/compound/2_4_6-Trimethylphenol. Accessed Feb. 9, 2021.

3.ii Butenedial/OH^- rate constant (k_1) vs. pH

The fitting of the rate constant k_1 as a function of pH is shown in Figure S11 below. As mentioned in Section 2, at constant pH, the reaction of dialdehydes with OH^- is an apparent first order rate law that is linearly dependent on the dialdehyde. In each experiment, pH was held constant with a carbonate buffer system and monitored with NMR. The decay of butenedial in four experiments at different pH was measured and a first-order linear fit was applied using Python's scipy package. Specifically, the lmfit library with the Levenberg-Marquardt algorithm was used to perform the least squares minimization. A Monte Carlo simulation was performed to derive the reported 95% confidence intervals on model runs. The extracted k_1 values from the model fit, reported for each experiment in Figure S11 below, were used to fit the empirical formulation, demonstrated in Section 3.2 of the main text.

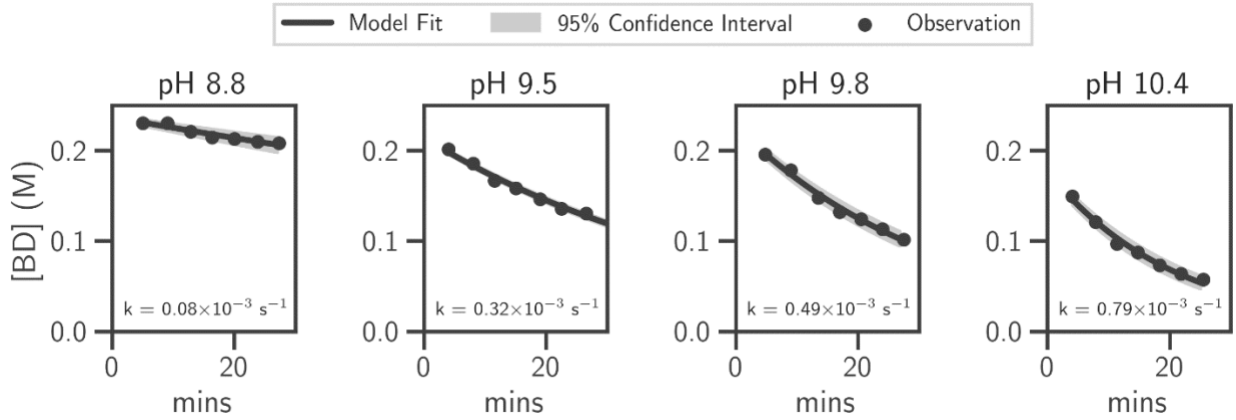

Figure S11. The loss of butenedial due to disproportionation reaction with OH^- is shown for four experiments at different pH. The pH was held constant and is shown above each panel. Measurements were performed with 1H-NMR. Modeled fits were performed with a linear regression of the natural logarithm of the concentration data. First-order rate constants (i.e., k_1) were extracted from the modeled fits and are shown on each panel. 95% confidence interval of the fitting is shown.

3.iii pH empirical fit

Experimental pH was observed to closely follow a curve of the form

$$pH(t) = \frac{a\ t}{b\ t + c}$$

in BD_NH_pH5 and BD_NH_pH8.5 observations. pH decrease is observed in glyoxal/NH_X reactions as well (Yu et al., 2011).

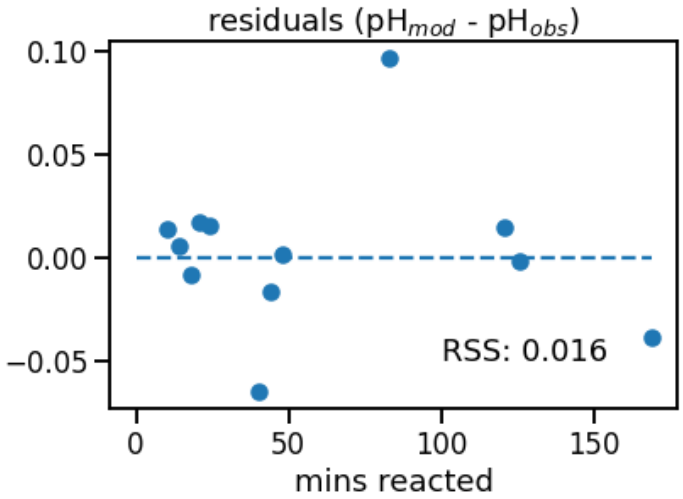

Figure S12. Residuals of median estimated and observed pH in BD_NH_pH5 measurements are shown below. There is not a clear trend in the residuals, which are all within 0.1 pH units.

3iii. Sensitivity of kinetic mechanism to NH_X estimation

As explained in Section 2 of the main text, NH_X was not explicitly measured and instead estimated through a 1:1 loss rate with butenedial (i.e., per butenedial lost, one NH_X is lost). This assumption will overestimate NH_X loss when butenedial is consumed by accretion reactions that do not additionally consume NH_X. The sensitivity of the mechanism to the NH_X estimation technique is assessed by comparing the parametrization against the other extreme scenario: constant NH_X, i.e., $NH_X(t) = NH_{X,0}$. The difference in the parameter estimates is a measure of the maximum attainable variability between NH_X estimation techniques.

$$S_i = \frac{|k_{i,0} - k_{i,1:1}|}{k_{i,1:1}}$$

The sensitivity (S) is calculated by taking the difference between parameter estimates from the constant NH_X (subscript 0) and 1:1 butenedial and NH_X loss (subscript 1:1) scenarios, relative to the estimate recorded for the 1:1 loss scenario. For example, a value of 1 indicates that difference in estimates is equal to the estimate. The estimates are taken from model fits to BD_NH_pH5 data.

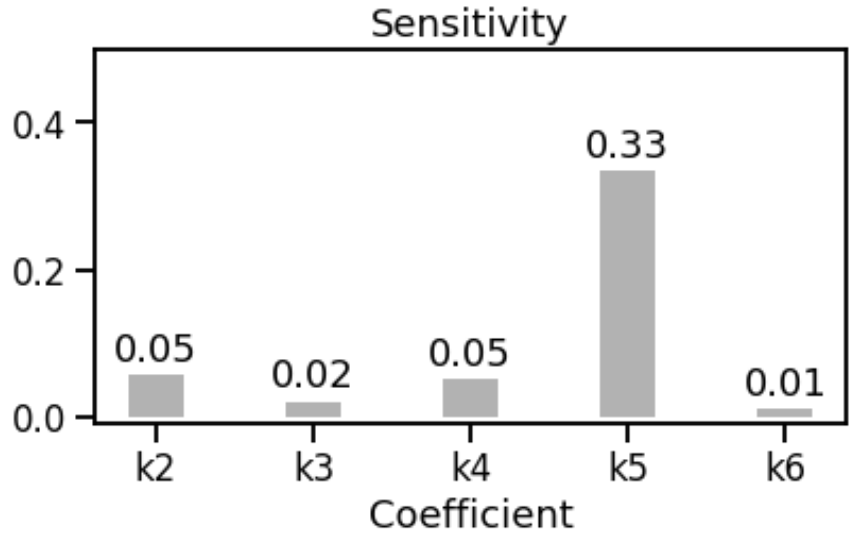

Figure S13. Sensitivities of the parameter estimates to NH_X estimation technique (1:1 NH_X:butenedial removal or constant NH_X). Most sensitivities are <0.05 the parameter estimate, indicating that those parameters (k_2, k_3, k_4, k_6) are not affected significantly by the NH_X estimation technique. k_5, i.e., removal of pyrrolinone through accretion reactions, is much more sensitive to the estimation technique. This may indicate that the pyrrolinone removal term is the least constrained of the parameters.

3iv. Assessment of reaction mechanism

The kinetic mechanism described in DE1-3 and Table 3 in the main text is evaluated through comparisons against measurements of butenedial taken from different experiments (BD_NH_pH3.6 and BD_NH_pH8.5). The pH and initial conditions of the experiments, described in Table S1, were taken as model inputs. Model outputs and experimental measurements of butenedial are shown in Figures S14 and S15 and generally indicate that the kinetic mechanism can predict butenedial loss in aqueous solutions containing ammonia at a range of pHs.

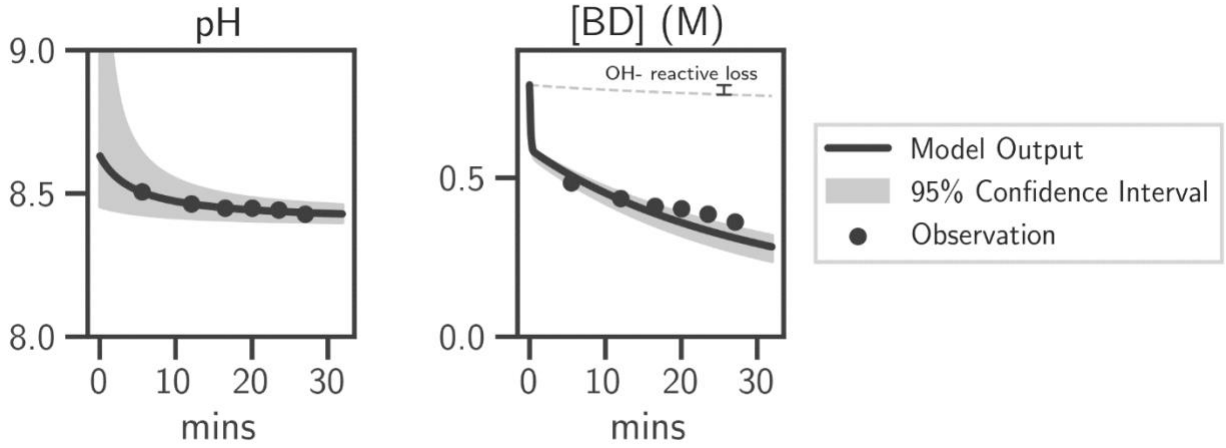

Figure S14. Experimental observations of BD_NH_pH8.5 against model outputs of the kinetic mechanism taken with the recorded pH and same initial conditions. pH was modeled with an empirical fit described in Equation. The initial pH conditions are poorly constrained by the empirical fit, although the median agrees with a starting pH of >8-9 witnessed with litmus paper. Butenedial is removed rapidly until all NH_X is consumed. The remaining butenedial decays at a slower pace through accretion reactions. Loss due to reaction with OH^- is shown to be a minor sink of butenedial at pH 8.5 compared to loss from reaction with NH_X and accretion reactions.

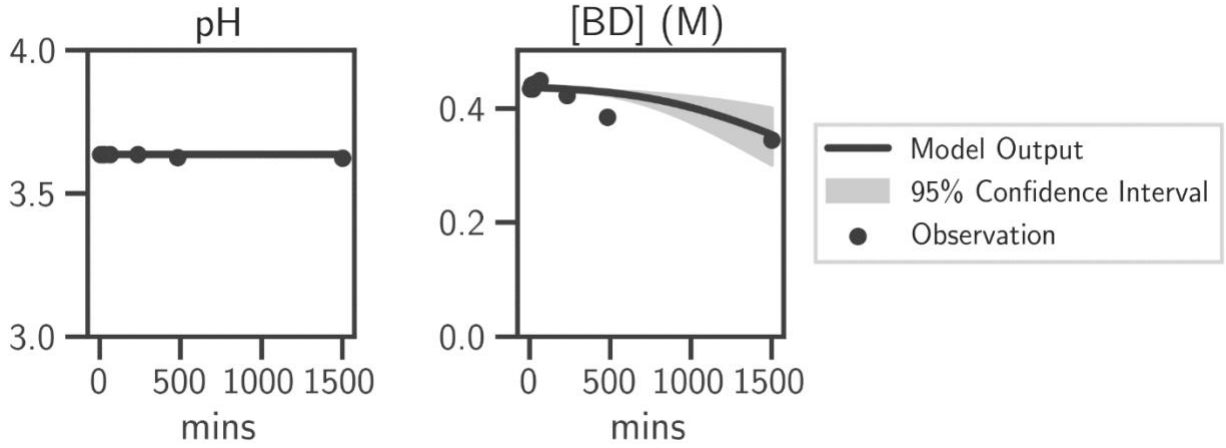

Figure S15. Experimental observations of BD_NH_pH3.6 against model outputs of the kinetic mechanism taken with the recorded pH and same initial conditions. pH was approximately

constant throughout the experimental run. Modeled butenedial agrees with butenedial measurements generally, with the exception of a slight overestimation compared to the measurement taken at ~500 minutes of reaction.

4 References

Bader, R. F. W.: Atoms in molecules : a quantum theory, Clarendon Press, Oxford., 1990.
Birdsall, A. W., Krieger, U. K. and Keutsch, F. N.: Electrodynamic balance–mass spectrometry of single particles as a new platform for atmospheric chemistry research, Atmos. Meas. Tech., 11(1), 33–47, https://doi.org/10.5194/amt-11-33-2018, 2018.
Birdsall, A. W., Hensley, J. C., Kotowitz, P. S., Huisman, A. J. and Keutsch, F. N.: Single-particle experiments measuring humidity and inorganic salt effects on gas-particle partitioning of butenedial, Atmos. Chem. Phys., 19(22), 14195–14209, https://doi.org/10.5194/acp-19-14195-2019, 2019.
Bocchi, V., Chierici, L., Gardini, G. P. and Mondelli, R.: On pyrrole oxidation with hydrogen peroxide, Tetrahedron, 26(17), 4073–4082, https://doi.org/10.1016/S0040-4020(01)93048-0, 1970.
Bordner, J. and Rapoport, H.: Synthesis of 2,2'-Bipyrroles from 2-Pyrrolinones [1a], J. Org. Chem., 30(11), 3824–3828, https://doi.org/10.1021/jo01022a053, 1965.
Capon, B., Guo, B.-Z., Kwok, F.-C. and Wu, Z.-P.: Some studies on the tautomerism of heterocyclic and homocyclic compounds, Pure and Applied Chemistry, 59(12), 1577–1584, https://doi.org/10.1351/pac198759121577, 1987.
Fratzke, A. R. and Reilly, P. J.: Thermodynamic and kinetic analysis of the dimerization of aqueous glyoxal, Int. J. Chem. Kinet., 18(7), 775–789, https://doi.org/10.1002/kin.550180705, 1986.
Hill, L., Imam, S., McNab, H. and O'Neill, W.: 3-Hydroxy-1H-pyrrole, Synthesis, 2009(15), 2535–2538, https://doi.org/10.1055/s-0029-1217422, 2009.
Wallace, M., Adams, D. J. and Iggo, J. A.: Titrations without the Additions: The Efficient Determination of p K_a Values Using NMR Imaging Techniques, Anal. Chem., 90(6), 4160–4166, https://doi.org/10.1021/acs.analchem.8b00181, 2018.
Yu, G., Bayer, A. R., Galloway, M. M., Korshavn, K. J., Fry, C. G. and Keutsch, F. N.: Glyoxal in Aqueous Ammonium Sulfate Solutions: Products, Kinetics and Hydration Effects, Environ. Sci. Technol., 45(15), 6336–6342, https://doi.org/10.1021/es200989n, 2011.